Hindawi
Contrast Media & Molecular Imaging
Volume 2018, Article ID 4535476, 14 pages
https://doi.org/10.1155/2018/4535476

Review Article

In Vivo and In Vitro Characteristics of Radiolabeled Vesamicol Analogs as the Vesicular Acetylcholine Transporter Imaging Agents

Kazuma Ogawa[1] **and Kazuhiro Shiba**[2]

[1]*Kanazawa University, Graduate School of Pharmaceutical Sciences, Kakuma-machi, Kanazawa, Ishikawa 920-1192, Japan*
[2]*Advanced Science Research Center, Kanazawa University, 13-1 Takara-machi, Kanazawa, Ishikawa 920-8640, Japan*

Correspondence should be addressed to Kazuhiro Shiba; shiba@med.kanazawa-u.ac.jp

Received 27 November 2017; Revised 3 April 2018; Accepted 2 May 2018; Published 13 June 2018

Academic Editor: Giorgio Biasiotto

The vesicular acetylcholine transporter (VAChT), a presynaptic cholinergic neuron marker, is a potential internal molecular target for the development of an imaging agent for early diagnosis of neurodegenerative disorders with cognitive decline such as Alzheimer's disease (AD). Since vesamicol has been reported to bind to VAChT with high affinity, many vesamicol analogs have been studied as VAChT imaging agents for the diagnosis of cholinergic neurodeficit disorder. However, because many vesamicol analogs, as well as vesamicol, bound to sigma receptors (σ_1 and σ_2) besides VAChT, almost all the vesamicol analogs have been shown to be unsuitable for clinical trials. In this report, the relationships between the chemical structure and the biological characteristics of these developed vesamicol analogs were investigated, especially the in vitro binding profile and the in vivo regional brain accumulation.

1. Introduction

Many clinical trials for early diagnosis of Alzheimer's disease by amyloid PET imaging have been reported [1–10]. Many researchers have reported that amyloid imaging is useful for early diagnosis of AD, but there have been many reports showing no significant association between the brain accumulation of amyloid imaging agents and the severity of dementia in AD [11–15]. Recently, there were many reports that tau imaging was useful for the diagnosis of the severity of dementia and early diagnosis of AD [16–20]. Evaluation of the diagnostic efficacy of tau imaging regarding AD will continue for several years. The onset of AD, which is a progressive neurological disease characterized by reduction in cognitive function and memory, is thought to be caused by a hypothesized amyloid cascade (Figure 1) [21]. Namely, (1) amyloid β (Aβ40 and Aβ42), which is produced by an abnormal cleavage of the amyloid precursor protein (APP) by β- and γ-secretase, is aggregated and accumulated extracellularly in cranial nerve cells. (2) Neurofibrillary tangles (NFTs) are formed by the accumulation of a tau protein phosphorylated excessively in the cytoplasm. (3) Nerve degeneration, neurologic function deficiency, and metabolism deficiency occur in the neuronal cell. (4) Neuronal cell death occurs, which causes the onset of AD. Abnormal accumulation of amyloid β based on the amyloid cascade supports the usefulness of amyloid imaging for early diagnosis of AD. On the contrary, studies of amyloid β immunotherapy showed that reduction of amyloid β plaques in patients with Alzheimer's disease did not prevent progressive neurodegeneration [22]. The amyloid β plaque is an antecedent marker of Alzheimer's disease [22], and amyloid imaging will not be useful to evaluate the therapeutic efficacy of AD treatment. Neuronal degeneration, neurologic function deficiency, and metabolic deficiency in the third step of the amyloid cascade are thought to be important internal molecular targets for the development of an imaging agent for the early diagnosis of neurodegenerative disorders with cognitive decline such as AD. Acetylcholine esterase inhibitors such as donepezil are commonly used for

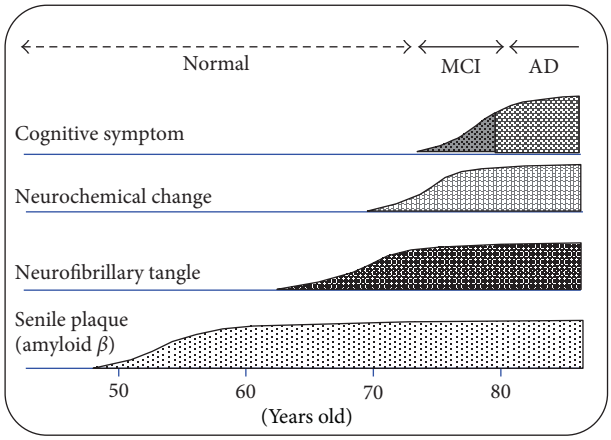

Figure 1: Process of the Alzheimer's disease onset.

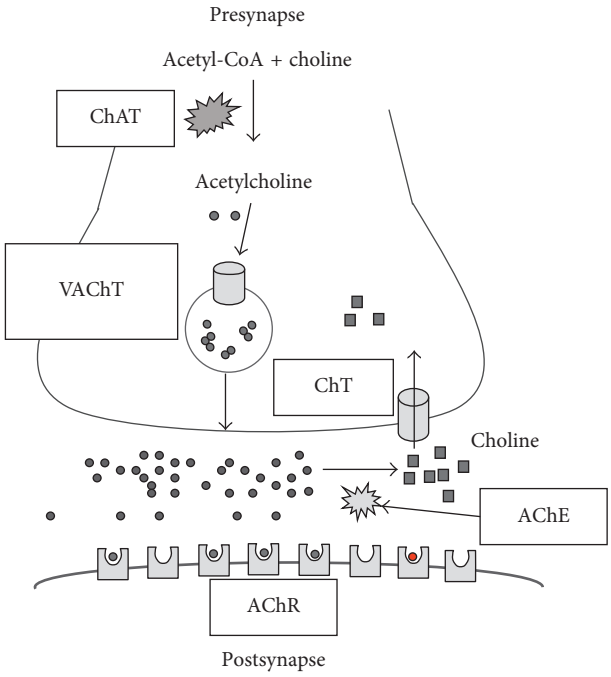

Figure 2: Schematic representation of a nerve terminal in acetylcholine neurotransmission. ChAT: choline acetyl transferase; VAChT: acetylcholine transporter; AChR: acetylcholine receptor; AChE: acetylcholine esterase; ChT: choline transporter.

treatment of cognitive dysfunction in AD [23, 24]. The dysfunction of cholinergic neurons is associated with AD symptoms such as cognitive dysfunction, memory impairment, and learning disorders [25]. Presynaptic cholinergic function, such as loss of choline acetyl transferase (ChAT), the enzyme for synthesis of acetylcholine (ACh) from choline and acetyl-coenzyme A, and the vesicular acetylcholine transporter (VAChT), the transporter for the accumulation of acetylcholine (ACh) inside the synaptic vesicles, is changed in AD [26, 27]. Thus, the internal molecules in the cholinergic nerve system will be suitable as the cranial molecular target of an imaging agent for early diagnosis of AD. There are five main molecular targets: choline acetyl transferase (ChAT), vesicular acetylcholine transporter (VAChT), choline transporter (ChT), acetylcholine esterase (AChE), and postsynaptic receptors in the cholinergic synaptic terminal (Figure 2). A small molecule compound binding to ChAT with high affinity has not yet been found, and only hemicholinium-3 (HC-3) with a positive electric charge as a small molecule compound binding to ChT, the transporter for reuptake of choline (Ch) released by ACh hydrolysis in the synaptic cleft, has been found, which makes the development of ChAT and ChT imaging agents difficult. A reduction in AChE activity in AD patients was shown by PET imaging using [^{11}C]MP4A and [^{11}C]PMP [28–31]. However, these AChE imaging agents, a selective substrate for AChE, show low stability in the blood, and quantitative measurement is thought to be difficult. Changes in presynaptic cholinergic functions, such as ChAT and VAChT activity in AD, are thought to be more significant than changes in postsynaptic cholinergic functions, such as the cholinergic muscarinic receptors (mAChR) [26, 27, 32]. Therefore, VAChT is an excellent in vivo target substrate for the early diagnosis of AD. Many vesamicol analogs have been developed as potential VAChT imaging agents for PET or SPECT, since vesamicol (2-(4-phenylpiperidino) cyclohexanol) was reported to bind to VAChT [33, 34]. However, many of the reported vesamicol analogs were shown to be insufficient for use as VAChT imaging agents due to binding to sigma receptors (σ_1 and σ_2) or low accumulation in brain in vivo. Many vesamicol analogs were developed with the aim of improving VAChT affinity and decreasing the affinity for sigma receptors (σ_1 and σ_2).

In this report, the biological characteristics of these developed vesamicol analogs were investigated, especially the in vitro binding profile and the in vivo regional brain accumulation. PET ligands for VAChT had been reviewed by Giboureau previously [35]. We tried to compare in vitro and in vivo characteristics of many VAChT ligands including these PET ligands under the same conditions as much as possible.

2. VAChT Imaging Agent Based on Vesamicol Analogs

The molecular structures of VAChT imaging agents based on vesamicol analogs are shown in Figure 3.

2.1. Vesamicol Analogs Based on Benzovesamicol

*2.1.1. 5-Iodobenzovesamicol (IBVM) (**1**).* Rogers et al. investigated the binding affinity of 84 vesamicol analogs to VAChT in an in vitro binding assay [36] and reported benzovesamicol as one of the vesamicol analogs binding to VAChT with a high affinity. Benzovesamicol (BV) is the vesamicol analog with a benzene ring in ring A of the vesamicol skeleton (Figure 3). The affinity ($IC_{50} = 50$ nM) of the racemate of BV to VAChT is similar to that ($IC_{50} = 40$ nM) of the racemate of vesamicol in the in vitro binding assay [36]. (−)-[^{123}I]-5-iodobenzovesamicol ((−)-[^{123}I]IBVM) (**1**), which has an iodine-123-labeled group at the 5th position of the benzene ring in ring A, was first developed as a potential

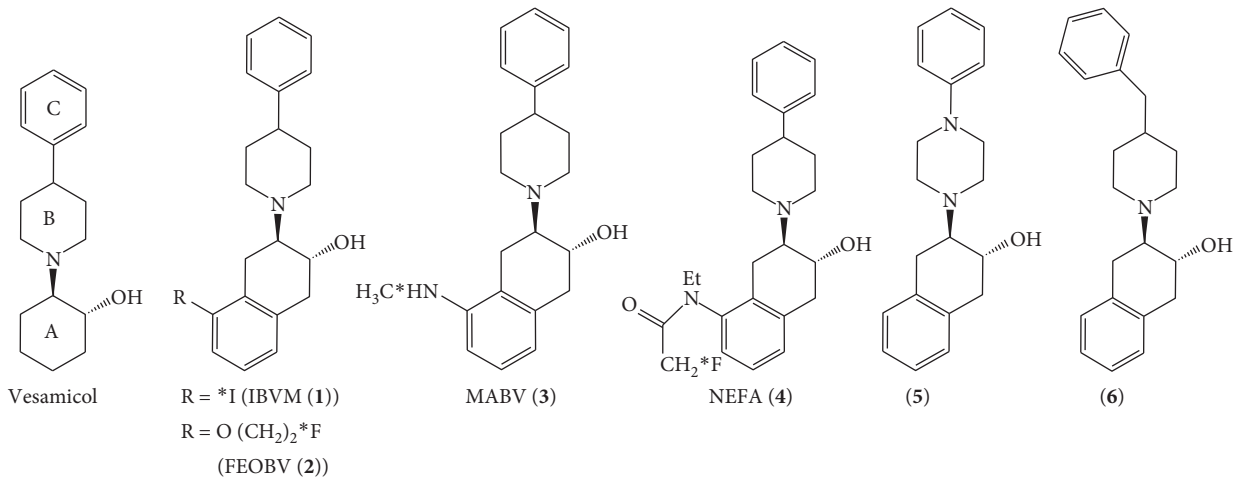

(a)

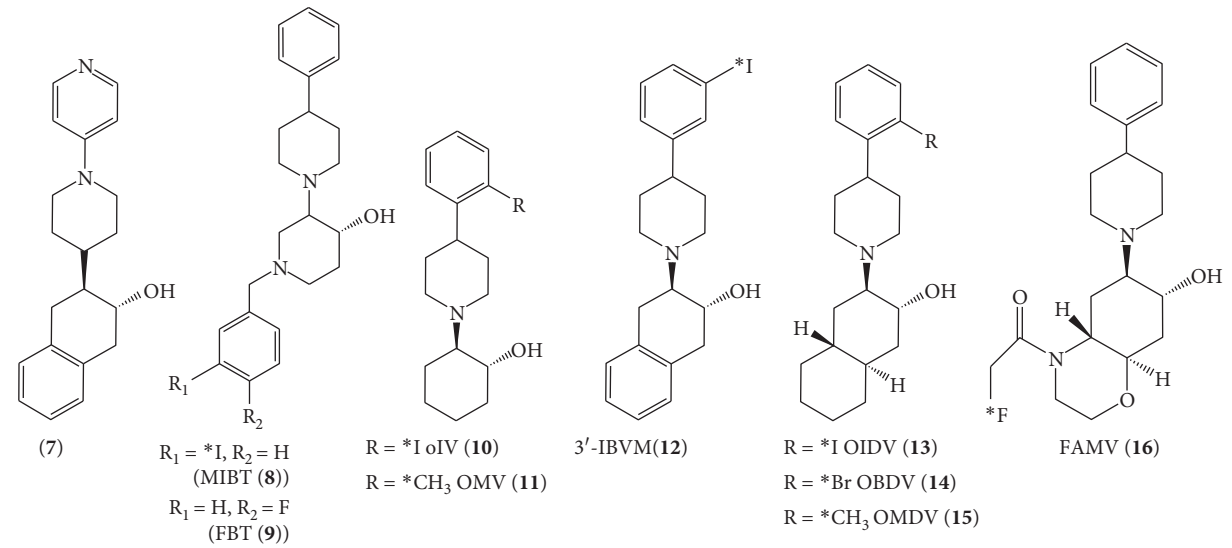

(b)

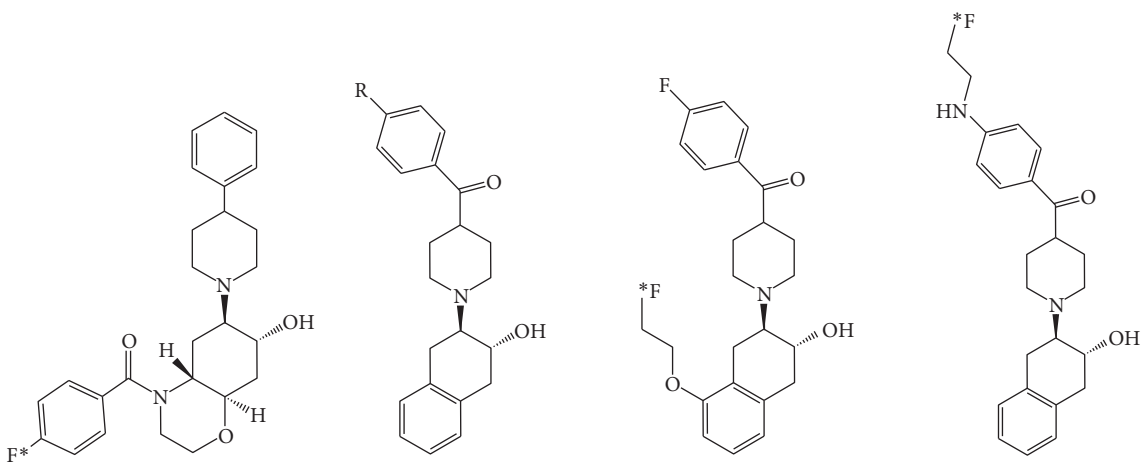

(c)

Figure 3: Molecular structures of vesamicol analogs. Benzovesamicol analogs: (**1**)–(**7**). Trozamicol analogs: (**8**) and (**9**). Vesamicol analogs with a radionuclide into the C ring: (**10**)–(**12**). Vesamicol analogs with alicyclic groups into the A ring: (**13**)–(**17**). Vesamicol analogs with a carbonyl group between the B ring and C ring: (**18**)–(**22**).

VAChT imaging agent. However, the affinity of IBVM to VAChT has not been reported [37, 38], and the accumulation of (−)-[^{123}I]IBVM (**1**) in the rodent brain may be insufficient for in vivo brain imaging for SPECT, considering the radiation dose and spatial resolution. The accumulation of (−)-[^{123}I] IBVM (**1**) in the cortex and striatum was 2.56 %ID/g and 6.26 %ID/g in mice 4 h after injection, respectively, and 0.30 % ID/g and 0.53 %ID/g in rats 2 h after injection, respectively [37]. The uptake of (−)-[^{123}I]IBVM (**1**) in the striatum is much higher than that in the cortex, and the ratio of the striatum to cortex for (−)-[^{123}I]IBVM (**1**) accumulation was 2.44 at 4 h after injection. Kuhl et al. extended to human use (−)-[^{123}I] IBVM (**1**) for SPECT (single-photon emission computed tomography). Several researchers showed that a decrease in (−)-[^{123}I]IBVM (**1**) binding was apparent in regional brain areas such as the temporal cortex, cingulate cortex, and parahippocampal-amygdaloid complex in AD [39, 40].

The human study using [^{123}I]IBVM-SPECT showed that a significant decrease in [^{123}I]IBVM (**1**) binding (47–62%) was apparent in AD subjects in the cingulate cortex and parahippocampal-amygdaloid complex [43].

*2.1.2. Fluoroethoxy-benzovesamicol (FEOBV) (**2**).* As a benzovesamicol analog for PET, [^{18}F]fluoroethoxy-benzovesamicol ([^{18}F]FEOBV (**2**)) was synthesized and investigated for regional brain distribution in mice by Mulholland et al. [44]. The binding affinity (Ki) of (−)-FEOBV (**2**) to VAChT and σ1 was 19.6 nM (PC12$^{A123.7}$ cells, which express human VAChT) and 209 nM (rat brain), respectively [45]. However, in the in vitro binding assay, vesamicol as a reference was not assessed simultaneously. The accumulation of [^{18}F]FEOBV (**2**) in the striatum in mice 5, 45, and 240 min after injection was 6.02, 8.09, and 7.29 %ID/g, and the accumulation of [^{18}F]FEOBV (**2**) in the cortex in mice 5, 45, and 240 min after injection was 5.00, 4.65, and 2.91 %ID/g, respectively [46]. Thus, the mouse brain uptake of [^{18}F]FEOBV (**2**) is insufficient for in vivo brain imaging with PET. The ratios of the striatum to cortex for [^{18}F] FEOBV (**2**) accumulation were 1.20, 1.74, and 2.51 after 5, 45, and 240 min injection, respectively. The in vivo human studies demonstrated that [^{18}F]FEOBV (**2**) is a reliable imaging tool for VAChT [47].

*2.1.3. Aminobenzovesamicol (−)-[^{11}C]-Methylaminobenzovesamicol ((−)-[^{11}C]MABV (**3**)) and (−)-[^{18}F]-N-ethyl-N-fluoroacetamidobenzovesamicol ((−)-[^{18}F]NEFA (**4**)).* As benzovesamicol analogs with the amino group, (−)-[^{11}C]-methylaminobenzovesamicol ((−)-[^{11}C]MABV (**3**)) [48] and (−)-[^{18}F]-*N*-ethyl-*N*-fluoroacetamidobenzovesamicol ((−)-[^{18}F] NEFA (**4**)) [49, 50] were reported. The accumulation of (−)-[^{11}C]MABV (**3**) in the striatum, the cortex, the hippocampus, and the cerebellum in mice 45 min after injection was 8.10, 3.99, 3.58, and 1.05 %ID/g, although the binding affinity (Ki) of (−)-[^{11}C]MABV (**3**) to VAChT and σ_1 and σ_2 receptors was not reported. The binding affinity (Ki) of (−)-[^{18}F]NEFA (**4**) to VAChT was 0.32 nM and was about 3-fold higher than that of vesamicol. The binding affinity (Ki) of (−)-[^{18}F]NEFA (**4**) to σ_1 and σ_2 receptors was not reported. The accumulation of (−)-[^{18}F]NEFA (**4**) in the rat whole brain 60 min after injection was 0.35 %ID/g.

2.1.4. Summary regarding Benzovesamicol Analogs. Although benzovesamicol (BV) has higher affinity and selectivity for VAChT than vesamicol, several benzovesamicol (BV) analogs were synthesized to improve VAChT affinity and to decrease the affinity for sigma receptors (σ_1 and σ_2). A BV analog with phenylpiperazine instead of phenylpiperidine in BV (**5**) [51, 52], a BV analog with benzylpiperidine instead of phenylpyridine (**6**), and a BV analog with pyridinyl piperidine instead of phenyl piperidine (**7**) showed a lower VAChT affinity than BV [53]. The affinity of **7** to the σ1 receptor increased.

2.2. Vesamicol Analogs Based on Trozamicol

*2.2.1. (+)-m-Iodobenzyltrozamicol (MIBT) (**8**).* The structure of *m*-iodobenzyltrozamicol (MIBT) (**8**) consists of a trozamicol skeleton, a compound with piperidine instead of cyclohexane in A ring, with an *m*-iodobenzyl group. The binding affinity of MIBT (**8**) to VAChT, σ_1, and σ_2 was 0.13 nM (*Torpedo californica*), 92 nM (Guinea pig membranes), and 190 nM (rat liver), respectively, and the binding affinity of vesamicol to VAChT, σ_1, and σ_2 was 2.0 nM (*Torpedo californica*), 26 nM (Guinea pig membranes), and 34 nM (rat liver), respectively [54]. (+)-MIBT (**8**) is the optical isomer of MIBT. The binding affinity of (+)-MIBT (**8**) to VAChT (Ki = 12.2 nM (rat brain)), σ1 (Ki = 8.4 nM (Guinea pig brain)), and σ2 (Ki = 40.4 nM (N18TG2 cell fused with septal neurons rat (σ_2)) and the binding affinity of (−)-vesamicol to VAChT (Ki = 26.6 nM), σ_1 (Ki = 37.6 nM), and σ_2 (Ki = 42.3 nM) were reported by Custers et al. [55]. (+)-*m*-[^{125}I]-iodobenzyltrozamicol ((+)-[^{125}I]MIBT (**8**)) accumulation in the rat brain was 0.57, 0.36, 0.27, and 0.15 %ID/g at 5, 30, 60, and 180 min after injection, respectively. The ratio of the striatum to cortex for (+)-[^{125}I]MIBT (**8**) accumulation was 1.73–2.34 at 180 min after injection. (+)-[^{125}I]MIBT (**8**) showed rapid clearance from blood. Pretreatment of rats with vesamicol (1.01 μmol/kg) decreased (+)-[^{125}I]MIBT (**8**) accumulation in the rat brain by 40% [56]. Coadministration of (+)-[^{125}I]MIBT (**8**) with haloperidol (0.5 μmol/kg), a known sigma receptor ligand, decreased (+)-[^{125}I]MIBT accumulation in the cortex and the cerebellum but increased (+)-[^{125}I]MIBT (**8**) accumulation in the striatum. In further studies, preinjection of spiperone (2 mg/kg), a known dopamine D_2 receptor ligand, increased (+)-[^{125}I]MIBT (**8**) accumulation in the striatum. The increase of (+)-[^{125}I]MIBT (**8**) accumulation in the striatum was thought to be caused by interaction between the dopaminergic nerve system and cholinergic nerve system [57]. A human SPECT study with (+)-[^{123}I]MIBT (**8**) was not performed, but (+)-[^{123}I]MIBT-SPECT study was performed using a female baboon [58, 59].

*2.2.2. (+)-p-Fluorobenzyltrozamicol (FBT) (**9**).* (+)-*p*-Fluorobenzyltrozamicol ((+)-FBT (**9**)) is a vesamicol analog having trozamicol with a *p*-fluorobenzyl group. The

Table 1: Binding affinity of vesamicol analogs for VAChT, σ_1, and σ_2.

	The ratio of vesamicol analogs (**1**–**22**) to vesamicol for Ki value			Tissue preparations for VAChT
	VAChT	σ_1	σ_2	
Vesamicol	1	1	1	—
Benzovesamicol (BV)	0.56	0.80	0.86	Rat brain membranes
Decalinvesamicol (DV)	0.50	2.75	0.31	Rat brain membranes
(−)-IBVM (**1**)*	—	—	—	—
(−)-FEOBV (**2**)** [45]	0.41	10.25	—	rVAChT-PC12 cell
(−)-MABV (**3**) [48]	—	—	—	—
(−)-NEFA (**4**) [49]	0.32	—	—	*Torpedo californica*
(**5**) [51]	1.17	22.84	11.38	rVAChT-PC12 cell
(**6**) [53]	0.49	3.19	0.54	rVAChT-PC12 cell
(**7**) [53]	0.14	0.44	2.30	rVAChT-PC12 cell
MIBT (**8**) [55]	0.065	3.54	5.59	*Torpedo californica*
(+)-MIBT (**8**) [55]	0.11	0.13	0.51	Rat brain membranes
FBT (**9**) [55]	0.25	0.04	0.66	Rat brain membranes
(+)-FBT (**9**) [60]	0.22	0.84	1.04	*Torpedo californica*
oIV(**10**) [62]	0.42	0.077	0.83	Rat brain membranes
(−)-oIV (**10**) [62]	1.15	0.83	1.32	Rat brain membranes
(−)-OMV (**11**) [63]	1.52	0.46	0.77	Rat brain membranes
3′-IBVM (**12**) [64]	0.21	5.75	1.37	*Torpedo californica*
OIDV (**13**) [65]	0.61	10.94	1.37	Rat brain membranes
(−)-OIDV (**13**) [66]	0.95	8.66	0.86	Rat brain membranes
OBDV (**14**) [67]	0.41	6.82	1.59	Rat brain membranes
OMDV (**15**) [68]	0.56	3.38	0.31	Rat brain membranes
FAMV (**16**) [69]	—	—	—	rVAChT-PC12 cell
FBMV (**17**) [70]	—	—	—	rVAChT-PC12 cell
(−)-FBBV (**18**) [71]	0.51	13.90	9.25	*Torpedo californica*
(−)-**19****	—	—	—	rVAChT-PC12 cell
(−)-TZ659 (**20**)**	—	—	—	rVAChT-PC12 cell
(−)-VAT (**21**)**	—	—	—	rVAChT-PC12 cell
(−)-**22****	—	—	—	rVAChT-PC12 cell

*The affinity of these vesamicol analogs for VAChT, σ1, and σ2 had not been reported. **The affinity of vesamicol, as a reference, for VAChT, σ1, and σ2 was not investigated by the same in vitro binding assay method.

binding affinity (Ki) of (+)-FBT (**9**) to VAChT, σ_1, and σ_2 was 0.22 nM (*Torpedo californica*), 21.6 nM (Guinea pig brain), and 35.9 nM (rat liver), respectively, and the binding affinity (Ki) of (−)-vesamicol to VAChT, σ_1, and σ_2 was 1.0 nM (*Torpedo californica*), 25.8 nM (Guinea pig brain), and 34.5 nM (rat liver), respectively [60]. Giboureau et al. reported that (+)-FBT (**9**) showed a 100- to 160-fold selectivity for the VAChT/σ_1/σ_2 receptors, while (−)-vesamicol showed a range from 25- to 35-fold selectivity for the VAChT/σ_1/σ_2 receptors [35]. The (+)-[^{18}F]FBT (**9**) accumulation in the rat brain was 0.82, 0.71, 0.59, 0.34, and 0.27 %ID/g at 5, 30, 60, 120, and 180 min after injection, respectively. The ratio of the striatum to cortex for (+)-[^{18}F]FBT (**9**) accumulation increased with time after (+)-[^{18}F]FBT (**9**) injection, and the striatum/cortex ratio was 1.89 at 180 min after injection [61]. Blocking studies using vesamicol, a VAChT ligand, or pentazocine, a selective σ_1 ligand, had not been reported. However, coadministration of (+)-[^{18}F]FBT (**9**) with haloperidol, a σ ligand and dopamine D_2 receptor ligand, increased (+)-[^{18}F]FBT (**9**) accumulation in the striatum. A radioactive metabolite of (+)-[^{18}F]FBT (**9**) that did not cross the blood-brain barrier (BBB) was observed in PET studies using rhesus monkeys [60, 61]. A human PET study with (+)-[^{18}F]FBT (**9**) has not been performed.

2.2.3. Summary regarding Trozamicol Analogs. The binding affinity of each trozamicol analog was investigated by a different method of the in vitro binding assay. Furthermore, different tissue membranes were used in the binding assay for VAChT or sigma receptors (σ_1 and σ_2). It is difficult to compare the value of the VAChT affinity of each trozamicol analog with the value of sigma receptors (σ_1 and σ_2) affinity. Thus, to compare all vesamicol analogs, the value of the affinity of vesamicol to VAChT and sigma receptors (σ_1 and σ_2) was used as the standard value in each binding assay in this report. Namely, the comparison between these vesamicol analogs was expressed as the ratio of the affinity of vesamicol analogs to the affinity of vesamicol to VAChT, σ_1, and σ_2, which were obtained by the same in vitro binding assay method (Table 1). The affinity and selectivity of MIBT to VAChT was superior to that of FBT [57]. (+)-FBT (**9**) showed a higher affinity and selectivity for VAChT than (−)-FBT [60]. The accumulation of (+)-[^{18}F]FBT (**9**) in the rat brain was higher than that of (+)-[^{125}I]MIBT (**9**) [56, 72]. However, the accumulation of (+)-[^{18}F]FBT (**9**) in the rat brain is lower than the expected brain accumulation based on the chemical structure of (+)-[^{18}F]FBT (**9**) [72]. Considering the radiation dose and spatial resolution, the

accumulation of (+)-[^{18}F]FBT (**9**) in the rat brain is insufficient for in vivo PET brain imaging.

2.3. Vesamicol Analogs That Incorporated a Radionuclide into the C Ring of Vesamicol

*2.3.1. (−)-o-Iodovesamicol ((−)-oIV (**10**)).* (−)-oIV (**10**) is a vesamicol analog having iodine at the *ortho*-position of the 4-phenylpiperidine moiety. It was reported that iodine at the *ortho*-position of the 4-phenylpiperidine moiety had no influence on affinity for VAChT and sigma receptors (σ_1 and σ_2) [62]. The binding affinity (Ki) of (−)-oIV (**10**) to VAChT, σ_1, and σ_2 was 15.0 nM (rat brain), 62.2 nM (rat brain), and 554 nM (rat liver), respectively, and the binding affinity (Ki) of (−)-vesamicol to VAChT, σ_1, and σ_2 was 13.0 nM (rat brain), 74.9 nM (rat brain), and 421 nM (rat liver), respectively. The accumulation of (−)-[^{125}I]oIV (**10**) in the rat brain was 1.50, 1.27, and 0.76 %ID/g at 30, 60, and 120 min after injection, respectively. The ratio of the striatum to cortex for (−)-[^{125}I]oIV (**10**) accumulation was 1.01 at 60 min after injection. The brain uptake of (−)-[^{125}I]oIV (**10**) was decreased by 60% by coadministration of (−)-[^{125}I]oIV (**10**) with vesamicol (0.5 μmol/kg) [73, 74]. In the unilateral nucleus basalis magnocellularis- (NBM-) lesioned rat, the accumulation of (−)-[^{125}I]oIV (**10**) in the ipsilateral cortex to the lesion was significantly lower than that in the contralateral cortex (about 17%) [74]. However, a human SPECT study with (−)-[^{123}I]oIV (**10**) was not performed.

*2.3.2. (−)-o-Methylvesamicol ((−)-OMV (**11**)).* (−)-OMV is a vesamicol analog having a methyl group at the *ortho*-position of the 4-phenylpiperidine moiety. The binding affinity (Ki) of (−)-OMV (**11**) to VAChT, σ_1, and σ_2 was 6.7 nM (rat brain), 33.7 nM (rat brain), and 266 nM (rat liver), respectively, and the binding affinity (Ki) of (−)-vesamicol to VAChT, σ_1, and σ_2 was 4.4 nM (rat brain), 73.8 nM (rat brain), and 346 nM (rat liver), respectively [63]. The (−)-[^{11}C]OMV (**11**) accumulation in the rat brain was 1.13, 0.98, and 0.80 %ID/g at 5, 30, and 60 min after injection, respectively [75]. As reported by Giboureau et al. [35], (−)-[^{11}C]OMV (**11**) was found to have the low brain uptake in primate (0.05% ID/mL) similar to (+)-[^{18}F]FBT (0.05–0.06% ID/mL) [61]. However, in the unilateral MBM-lesioned rhesus monkeys, the accumulation of (−)-[^{11}C]OMV (**11**) in the ipsilateral cortex to the lesion was significantly lower than that in the contralateral cortex. The reduction of the uptake of (−)-[^{11}C]OMV (**11**) (27.5%) in the ipsilateral cortex to the lesion was greater than that of [^{11}C]SA4503 (19.9%) [76]. A human SPECT study with (−)-[^{11}C]OMV (**11**) was not performed.

*2.3.3. 3′-Iodobenzovesamicol (3′-IBVM (**12**)).* 3′-IBVM is a benzovesamicol analog with a 4-(3-iodophenyl)piperidine moiety [64]. The binding affinity (Ki) of 3′-IBVM (**12**) to VAChT, σ_1, and σ_2 was 2.0 nM (*Torpedo californica*), 70.3 nM (rat brain), and 43.6 nM (Guinea pig brain), respectively. The accumulation of 3′-[^{125}I]IBVM (**12**) in the striatum and the cortex was 0.69 %ID/g and 0.57 %ID/g in rats 30 min after injection and 0.61 %ID/g and 0.38 %ID/g in the rat brain 60 min after injection, respectively. The ratio of the striatum to cortex for 3′-[^{125}I]IBVM (**12**) accumulation was 1.21 and 1.61 at 30 and 60 min after injection, respectively. The accumulation of 3′-[^{125}I]IBVM (**12**) in the striatum and the cortex was decreased by 28 and 70% by coadministration of 3′-[^{125}I]IBVM (**12**) with haloperidol (0.5 μmol/kg), respectively.

2.3.4. Summary of Vesamicol Analogs That Incorporated Halogen or Methyl Group in 4-Phenylpiperidine. Iodine at the *ortho*-position of the 4-phenylpiperidine moiety of vesamicol has no influence on the affinity for VAChT and decreased the affinity for sigma receptors (σ_1 and σ_2) [62]. Iodine at the *meta*-position of the 4-phenylpiperidine moiety of benzovesamicol has no influence on the affinity for VAChT and sigma receptors (σ_1 and σ_2) [64]. An (−)-enantiomer of vesamicol analogs, which has a halogen or a methyl group in 4-phenylpiperidine and an (−)-enantiomer of vesamicol, showed a higher affinity for VAChT than an (+)-enantiomer [62, 63]. (−)-oIV (**10**) [74] and (−)-OMV (**11**) [75] showed a high brain uptake in rats. 3′-IBVM (**12**) [76] showed lower brain uptake in rats than (−)-oIV (**10**) and (−)-OMV (**11**).

2.4. Vesamicol Analogs That Incorporated Alicyclic Groups into the A Ring of Vesamicol

*2.4.1. (−)-o-Iodo-trans-decalinvesamicol ((−)-OIDV (**13**)).* Decalinvesamicol (DV) showed the highest affinity for VAChT among 84 vesamicol analogs investigated by Rogers et al. (−)-OIDV (**13**) is a vesamicol analog having a decalin skeleton (as A ring) and a 4-(2-iodophenyl)piperidine moiety. The binding affinity (Ki) of (−)-OIDV (**13**) to VAChT, σ_1, and σ_2 was 22.1 nM (rat brain), 168 nM (rat brain), and 59.9 nM (rat liver), respectively. The ratio of the striatum to cortex for (−)-[^{123}I]OIDV (**13**) accumulation was 1.20 at 60 min after injection. The rat brain uptake of (−)-[^{123}I]OIDV (**13**) was decreased by 71–73% by coadministration of (−)-[^{123}I]OIDV (**13**) with vesamicol (0.25 μmol). (−)-[^{123}I]OIDV (**13**) was distributed in characteristically VAChT-rich regions, such as the cortex, striatum, diagonal band, amygdaloid nucleus, and trigeminal and facial nucleus [65, 66, 77].

*2.4.2. o-Bromo-trans-decalinvesamicol ((−)-OBDV (**14**)).* OBDV is a vesamicol analog having a decalin skeleton (as A ring) and a 4-(2-bromophenyl)piperidine moiety [67]. The binding affinity (Ki) of OBDV (**14**) to VAChT, σ_1, and σ_2 was 13.8 nM (rat brain), 150.7 nM (rat brain), and 137.5 nM (rat liver), respectively, and the binding affinity (Ki) of vesamicol to VAChT, σ_1, and σ_2 was 33.9 nM (rat brain), 22.1 nM (rat brain), and 86.7 nM (rat liver), respectively. The accumulation of [^{77}Br]OBDV (**14**) in the striatum was 0.59 and 0.53 %ID/g in rats 30 and 60 min after injection, respectively, and the accumulation of [^{77}Br]OBDV (**14**) in the cortex was 0.52 and 0.50 %ID/g in rats 30 and 60 min after injection,

respectively. The ratio of the striatum to cortex for [^{77}Br]OBDV (**14**) accumulation was 1.13 at 30 min after injection. The rat brain uptake of [^{77}Br]OBDV (**14**) was remarkably decreased by 60% by coadministration of [^{77}Br]OBDV (**14**) with vesamicol (0.25 μmol). On the contrary, coadministration of (+)-pentazocine or (+)-3-PPP had no significant influence on the accumulation of [^{77}Br]OBDV (**14**) in the rat brain.

*2.4.3. o-Methyl-trans-decalinvesamicol (OMDV (**15**)).* OMDV is a vesamicol analog having a decalin skeleton (as A ring) and a 4-(2-methylphenyl)piperidine moiety [68]. The binding affinity (Ki) of OMDV (**15**) to VAChT, σ_1, and σ_2 was 11.9 nM (rat brain), 70.3 nM (rat brain), and 43.6 nM (rat liver), respectively, and the binding affinity (Ki) of vesamicol to VAChT, σ_1, and σ_2 was 21.1 nM (rat brain), 20.8 nM (rat brain), and 139 nM (rat liver), respectively. The accumulation of [^{11}C]OMDV (**15**) in the cerebrum was 0.65 and 0.44 %ID/g in the rat brain 30 and 60 min after injection, respectively. The ratio of the striatum to cortex for [^{11}C]OMDV (**15**) accumulation was 1.11 at 30 min after injection. A PET/CT study using [^{11}C]OMDV (**15**) showed that the accumulation of [^{11}C]OMDV (**15**) in the rat brain was markedly decreased by 60% by coadministration of 0.25 μmol of vesamicol.

*2.4.4. Morpholinovesamicol Analogs 2-[^{18}F]fluoroacetyl morpholinovesamicol ([^{18}F]FAMV (**16**)) [69] and 4-[^{18}F]fluorobenzoyl morpholinovesamicol ([^{18}F]FBMV (**17**)) [70].* The binding affinity (Ki) of FAMV (**16**) to VAChT and σ receptors was 39.9 nM (PC12$^{A123.7}$ cells, which express rat VAChT) and >1500 nM (rat liver), respectively. FAMV (**16**) showed about 30-fold lower affinity than vesamicol. The accumulation of [^{18}F]FAMV (**16**) in the rat whole brain 60 min after injection was 0.35 %ID/g. The binding affinity (Ki) of FBMV (**17**) to VAChT and σ receptors was 27.5 nM (PC12$^{A123.7}$ cells, which express rat VAChT) and >3000 nM (rat liver), respectively. FBMV (**17**) showed about 2.4-fold lower affinity than (−)-vesamicol. FBMV (**17**) showed a higher selectivity to VAChT affinity than (−)-vesamicol because FBMV (**17**) showed lower affinity for σ receptors than (−)-vesamicol. The accumulation of [^{18}F]FBMV (**17**) in the rat whole brain 60 min after injection was 0.1 %ID/g.

2.4.5. Summary of Vesamicol Analogs That Incorporated Alicyclic Groups into the A Ring of Vesamicol. Decalinvesamicol ((−)-OIDV (**13**) [66], OBDV (**14**) [67], and OMDV (**15**)) [68] showed a higher affinity to VAChT than morpholinovesamicol analogs (FAMV (**16**) and FBMV (**17**)). On the contrary, morpholinovesamicol analogs showed a higher selectivity to VAChT affinity than decalinvesamicol. The accumulation of radiolabeled decalinvesamicol analogs in the rat brain was higher than that of [^{18}F]morpholinovesamicol analogs. However, radiolabeled decalinvesamicol analogs showed a lower brain uptake in rats than (−)-oIV (**10**) and (−)-OMV (**11**). The ratio of the striatum to cortex for [^{18}F]morpholinovesamicol analogs (3.4–4.5) accumulation was higher than that of radiolabeled decalinvesamicol analogs (1.1–1.2).

2.5. Vesamicol Analogs That Incorporated a Carbonyl Group between the B Ring and C Ring of Benzovesamicol

*2.5.1. (−)-trans-2-Hydroxy-3-(4-(4-fluorobenzoyl)piperidino) tetralin ((−)-FBBV (**18**)).* The affinity (Ki) of (−)-FBBV (**18**) to VAChT, σ_1, and σ_2 was 4.1 nM, 658.6 nM, and 319.23 nM, respectively [71, 78]. (−)-FBBV (**18**) displayed a 2-fold lower affinity for VAChT than vesamicol (Ki = 2.0 nM); furthermore, (−)-FBBV (**18**) displayed significantly lower affinity for VAChT than (+)-FBT (**9**) (Ki = 0.22 nM). However, (−)-[^{18}F]FBBV (**18**) displayed significantly lower affinity for σ_1 and σ_2 than vesamicol (Ki = 25.8 nM (σ_1) and Ki = 34.5 nM (σ_2)). The brain uptake of (−)-[^{18}F]FBBV (**18**) in rats was 0.823, 0.226, 0.124, and 0.095 %ID/g at 5, 30, 60, and 120 min after injection, respectively. (−)-[^{18}F]FBBV (**18**) displayed a low brain uptake in rats. The accumulation ratios of the striatum to cortex were 1.39, 1.36, and 1.09 at 30, 60, and 120 min after injection, respectively. The accumulation of (−)-[^{18}F]FBBV (**18**) in the rat brain is insufficient for in vivo brain imaging for PET.

*2.5.2. (−)-(3-(Hydroxy-1,2,3,4-tetrahydronaphthalen-2-yl) piperidin-4-yl)(4-methoxyphenyl)methanone (**19**).* The affinity (Ki) of (−)-**19** to VAChT, σ1, and σ2 was 1.6 nM (PC12$^{A123.7}$ cells which express human VAChT), 62.1 nM (Guinea pig brain), and 2,586 nM (rat liver), respectively [79, 80]. However, in the in vitro binding assay, vesamicol as a reference was not assessed simultaneously. The brain uptake of (−)-[^{11}C]**19** in rats was 0.560, 0.337, and 0.201 % ID/g at 2, 30, and 60 min after injection, respectively. The accumulation of (−)-[^{11}C]**19** in the striatum, cortex, and cerebellum at 30 min after injection was 0.546, 0.331, and 0.317 %ID/g, respectively. The accumulation ratios of the striatum to cortex (ST/CTX) and the striatum to cerebellum (ST/CBL) were 1.65 and 1.72, respectively.

*2.5.3. (−)-(1-(3-Hydroxy-1,2,3,4-tetrahydronaphthalen-2-yl) piperidin-4-yl)(4-(methylamino)phenyl)methanone ((−)-TZ659 (**20**)).* The affinity (Ki) of (−)-TZ659 (**20**) to VAChT, σ_1, and σ_2 was 0.78 nM (PC12$^{A123.7}$ cells which express human VAChT), 992 nM (Guinea pig brain), and 11443 nM (rat liver), respectively [81, 82]. (−)-TZ659 (**20**) displayed a 3.5-fold higher affinity for VAChT than (−)-FBBV (**16**) and displayed a significantly lower affinity for σ_1 and σ_2 than (−)-FBBV (**20**) [71]. The affinity of vesamicol to VAChT, σ_1, and σ_2 as a reference was not investigated by the same in vitro binding assay method. The accumulation levels of (−)-[^{11}C]TZ659 (**20**) in the striatum, cortex, and cerebellum at 30 min after injection were 0.593, 0.262, and 0.157 %ID/g, respectively. The accumulation ratios of the striatum to cortex (ST/CTX) and the striatum to cerebellum (ST/CBL) were 2.26 and 3.78, respectively [81]. PET studies of (−)-[^{11}C]TZ659 (**20**) in a male cynomolgus monkey were performed.

(−)-[^{11}C]TZ659 (**20**) displayed high accumulation in the striatum and low accumulation in the cerebellum [82].

*2.5.4. (−)-(1-(8-(2-Fluoroethoxy)-3-hydroxy-1,2,3,4-tetrahydronapthalen-2-yl)piperin-4yl)(4-fluorophenyl)methanone ((−)-VAT (**21**)) [83].* (−)-VAT (**21**) is a vesamicol analog that incorporated the 2-fluoroethoxy group into the 8th position of a tetrahydronapthalene skeleton of (−)-FBBV (**18**). The affinity (Ki) of (−)-VAT (**21**) to VAChT, σ_1, and σ_2 was 0.59 nM (PC12$^{A123.7}$ cells which express human VAChT), >10,000 nM (Guinea pig brain), and >10,000 nM (rat liver), respectively. (−)-VAT (**21**) displayed a 4.6-fold higher affinity for VAChT than FBBV (**18**) and displayed a significantly lower affinity for σ_1 and σ_2 than FBBV (**18**). However, the affinity of vesamicol to VAChT obtained by a different binding assay method was used as a reference. The brain uptake levels of (−)-[^{18}F]VAT (**21**) in rats were 0.684, 0.482, 0.425, and 0.409 %ID/g at 5, 30, 60, and 120 min after injection, respectively. The accumulation ratios of the striatum to cortex (ST/CTX) and the striatum to cerebellum (ST/CBL) were about 2.0 and 2.8 at 60 min after injection, respectively. PET studies of (−)-[^{18}F]VAT (**21**) in a male cynomolgus monkey were performed. (−)-[^{18}F]VAT (**21**) displayed high accumulation in the striatum and low accumulation in the cerebellum.

*2.5.5. (−)-(4-((2-Fluoroethyl)amino)phenyl)(1-(3-hydroxy-1,2,3,4-tetrahydronaphthalen-2-yl)piperidin-4-yl)methanone (**22**).* **22** is a vesamicol analog that incorporated the fluoroethyl amino group instead of the methylamino group into (−)-TZ659 (**20**) [84]. The affinity (Ki) of (**22**) to VAChT, σ1, and σ2 was 0.31 nM (PC12$^{A123.7}$ cells which express human VAChT), 1,870 nM (Guinea pig brain), and 5,480 nM (rat liver), respectively. PET studies of (−)-[^{18}F]**22** in a male cynomolgus macaque were performed. (−)-[^{18}F]**22** displayed high accumulation in the striatum and low accumulation in the cerebellum.

2.5.6. Summary of Vesamicol Analogs That Incorporated a Carbonyl Group between the B Ring and C Ring of Benzovesamicol. Benzovesamicol analogs that incorporated a carbonyl group displayed low affinity for sigma receptors (σ_1 and σ_2). These compounds (**12** and **16**–**21**) displayed a high selectivity for VAChT over sigma receptors (σ_1 and σ_2). However, because the affinity of vesamicol, as a reference, for VAChT, σ_1, and σ_2 and the affinity of sigma ligands such as pentazocine (σ_1) and DTG (σ_2), as a reference, for σ_1 and σ_2 were not investigated by the same in vitro binding assay method, it is difficult to compare between other vesamicol analogs (**1**–**17**) and these compounds (**18**–**22**) regarding the affinity for VAChT and sigma receptors (σ_1 and σ_2). These compounds (**18**–**22**) displayed low accumulation in the brain against the physicochemical characteristics such as molecular weight (MW = 354–405) and lipophilicity (ALog *D* or Log *P* = 2–3) [71, 81, 83, 84]. Tu et al. reported that the accumulation of (−)-[^{11}C]TZ659 (**20**) in the brain increased 2.2-fold by pretreatment with cyclosporine A (CycA), which inhibits a P-glycoprotein related to the drug excretion mechanism, 30 min prior to injection of a radiotracer [83]. On the contrary, 1-(4-[^{18}F]fluorobenzyl)-4-[(tetrahydrofuran-2yl)methyl]piperizine, which displayed a high brain uptake as a σ_1 receptor ligand, was unaffected by pretreatment with CycA [81]. These results showed that (−)-[^{11}C]TZ659 (**20**) was a substrate of CycA with low affinity, and the low accumulation of (−)-[^{11}C]TZ659 (**20**) in the brain was caused by CycA into the blood-brain barrier (BBB).

3. Discussion

3.1. Cholinergic Nerve Systems. The cholinergic system includes the following three main cholinergic pathways [85–90]: (1) numerous cholinergic neurons in the basal forebrain, which supply cholinergic projections throughout the cerebral cortex, the forebrain limbic structures, the diagonal band nucleus, the amygdala, and the hippocampus, (2) the mesopontine regions including the laterodorsal tegmental nucleus and the pedunculopontine nucleus, which project to the forebrain, the thalamus, the hypothalamus, the cerebellar nucleus, and the brainstem, and (3) populations of cholinergic interneurons in the striatum. Cholinergic neurons in the basal forebrain and the mesopontine regions are closely associated with cognition, learning, and memory functions. Cholinergic neurons in the striatum do not project beyond the borders of the striatum. It is important to investigate the change of the cholinergic nerve system in the cerebral cortex, the forebrain limbic structures, the diagonal nucleus, the amygdala, the hippocampus, the thalamus, the hypothalamus, and the cerebellar nucleus in comparison with the striatum in order to diagnose AD early by a VAChT imaging agent.

3.2. Binding Affinity of Vesamicol Analogs for VAChT, σ_1, and σ_2. It is difficult to compare between vesamicol analogs (**1**–**22**) because the affinity of vesamicol, as a reference, to VAChT, σ_1, and σ_2 was not investigated by the same in vitro binding assay method. In this report, the affinity of vesamicol analogs (**1**–**22**) to VAChT, σ_1, and σ_2 was compared with that of vesamicol as a reference (Table 1). (±)-MIBT (**8**) displayed a high affinity and high selectivity for VAChT using *Torpedo californica* as tissue preparations. However, Custers et al. reported that (+)-MIBT (**8**), FBT (**7**), and oIV (**10**) displayed higher affinity for σ_1 and σ_2 than vesamicol by the same in vitro binding assay method. OIDV (**13**), OBDV (**14**), and 3′-IBVM (**12**) displayed higher affinity for VAChT and lower affinity for σ_1 and σ_2 than vesamicol. (−)-FBBV (**18**) displayed the lowest affinity for σ_1 and σ_2. Vesamicol analogs (**19**–**22**), which incorporated a carbonyl group between the B ring and C ring, and (−)-FBBV (**18**) are expected to display low affinity for σ_1 and σ_2. Finally, to investigate the affinity of vesamicol analogs to VAChT, σ_1, and σ_2, it is necessary that vesamicol and novel vesamicol analogs for VAChT, σ_1, and σ_2 were assayed by the same in vitro binding assay simultaneously.

3.3. Distribution of VAChT in Cholinergic Neurons. The nerve terminal consists of presynaptic and postsynaptic neurons. The regional distribution of VAChT situated at presynaptic

Table 2: Accumulation of vesamicol analogs (**1**–**22**) in the striatum and cortex and the ratio of the striatum to cortex (ST/CTX) for radiolabeled vesamicol analogs accumulation.

	%ID/g		ST/CTX	Animal	Molecular weight	Partition coefficient
	Cortex	Striatum				
[^{3}H]vesamicol [74]	0.68 (60 min)	0.74 (60 min)	1.09 (60 min)	Rats	259	1.40*
Benzovesamicol	—	—	—	—	307	2.44*
[^{123}I]IBVM (**1**) [37, 42]	2.56 (240 min) 0.3 (120 min)	6.26 (240 min) 0.53 (120 min)	2.45 (240 min) 1.77 (120 min)	Mice Rats	429	— —
(−)-[^{18}F]FEOBV (**2**) [46]	4.65 (45 min)	8.09 (45 min)	1.74 (45 min)	Mice	368	—
(−)-[^{11}C]MABV (**3**) [48]	3.99 (45 min)	8.1 (45 min)	2.6 (75 min)	Mice	336	—
(−)-[^{18}F]NEFA (**4**) [49]	—	—	2.5–3 (50 min)	Monkeys	406	—
(+)-[^{125}I]MIBT (**8**) [56]	0.40 (120 min)	0.67 120 min)	1.68 (120 min)	Rats	474	—
(+)-[^{18}F]FBT (**9**) [72]	0.58 (60 min)	0.74 (60 min)	1.28 (60 min)	Rats	367	1.99*
(−)-[^{125}I]oIV (**10**) [74]	1.55 (60 min)	1.57 (60 min)	1.01 (60 min)	Rats	383	2.15**
(−)-[^{11}C]OMV (**11**) [75]	1.16 (30 min)	1.07 (30 min)	0.92 (30 min)	Rats	272	—
3′-[^{125}I]IBVM (**12**) [64]	0.38 (60 min)	0.61 (60 min)	1.61 (60 min)	Rats	431	—
(−)-[^{123}I]OIDV (**13**) [66]	0.62 (30 min)	0.63 (30 min)	1.02 (30 min)	Rats	435	2.46**
[^{77}Br]OBDV (**14**) [67]	0.52 (30 min)	0.59 (30 min)	1.13 (30 min)	Rats	389	2.93**
[^{11}C]OMDV (**15**) [68]	0.57 (60 min)	0.72 (60 min)	1.26 (60 min)	Rats	326	2.37**
[^{18}F]FAMV (**16**) [69]	—	—	4.5 (60 min)	Rats	361	1.88
[^{18}F]FBMV (**17**) [70]	0.09 (60 min)	0.17 (60 min)	3.4 (60 min)	Rats	423	2.10
(−)-[^{18}F]FBBV (**18**) [71]	—	—	1.36 (60 min)	Rats	352	2.99*
(−)-[^{11}C]**19** [80]	0.331 (30 min)	0.546 (30 min)	1.65 (30 min)	Rats	364	—
(−)-[^{11}C]TZ659 (**20**) [81]	0.262 (30 min)	0.593 (30 min)	2.26 (30 min)	Rats	363	2.61*
(−)-[^{18}F]VAT (**21**) [83]	—	—	4.19 (60 min)	Rats	414	3.45*
(−)-[^{18}F]**22** [84]	—	—	1.76 (60 min)	Monkeys	395	2.91*

*Calculated value (Log *P*) at pH 7.4 by ACD/Laboratories, version 7.0 (Advanced Chemistry Development, Inc., Canada). **Log $P_{o/w} = \log_{10}$ (radioactivity in *n*-octanol/radioactivity in 0.1 M phosphate buffer (pH = 7.4)).

cholinergic nerve terminals is similar to that of acetylcholine receptors situated at the postsynapses of cholinergic nerve terminals. Muscarinic acetylcholine (M_1–M_5) receptors (mAChR (M_1–M_5)) are found in high density in the cerebral cortex, striatum, diagonal band, hippocampus, amygdala, anterior and intralaminar nuclei of the thalamus, granule and purkinje cell layers of the cerebellum, and motor nuclei of the cranial nerves [91–93]. The nicotinic receptor is widely distributed in the anteroventral nucleus of the thalamus [94]. Therefore, VAChT-rich presynaptic cholinergic nerve terminals were thought to be widely distributed in various brain regions, including the cerebral cortex, striatum, diagonal band, hippocampus, thalamus, amygdaloid nucleus, cerebellum, and nuclei of cranial nerves. The mAChR concentrations in the striatum are approximately 1.67-fold higher than those in the cerebral cortex. Table 2 shows the accumulation of vesamicol analogs (**1**–**22**) in the striatum and cortex and the ratio of the striatum to cortex (ST/CTX) for radiolabeled vesamicol analogs. CNS radioligands need to accumulate in the brain through the BBB. The CNS radioligands are required to have 2-3 as the value of the log of the octanol-water partition coefficient (Log *P*) and be less than 500 as molecular weight (MW) as their chemical characteristics to penetrate the BBB [95, 96]. The vesamicol analogs (**1**–**22**) except for (−)-VAT (**21**) displayed physicochemical properties such as molecular weight (MW = 272–474) and lipophilicity (Log *P* = 2-3). (−)-oIV (**10**) and (−)-OMV (**11**) displayed high brain uptake in rat. However, other vesamicol analogs displayed low brain uptake in rats or mice against the physicochemical properties. The low brain uptake of vesamicol

Table 3: The ratio of binding affinity (Ki) of enantiomers of vesamicol analogs for VAChT, σ_1, and σ_2 receptors ((−)-body/(+)-body).

	The ratio of binding affinity (Ki) of enantiomers of vesamicol analogs for VAChT, σ1, and σ2 receptors ((−)-body/(+)-body)			Tissue preparations for VAChT
	VAChT	σ_1	σ_2	
Vesamicol [55]	0.034	4.88	1.12	Rat brain membranes
FEOBV (**2**) [45]	0.344	0.78	—	rVAChT-PC12 cell
MIBT (**8**) [55]	39.6	0.23	1.45	Rat brain membranes
FBT (**9**) [60]	72.7	1.03	3.05	*Torpedo californica*
oIV (**10**) [62]	0.063	4.29	2.80	Rat brain membranes
OMV (**11**) [63]	0.30	3.15	1.22	Rat brain membranes
OIDV (**13**) [66]	0.28	0.53	0.59	Rat brain membranes
FBBV (**18**) [71]	0.038	3.54	1.15	*Torpedo californica*
19** [80]	0.047	0.47	1.74	rVAChT-PC12 cell
TZ659 (**20**) [81]	0.041	0.85	1.47	rVAChT-PC12 cell
VAT (**21**) [71]	0.045	1.0	>1.28	rVAChT-PC12 cell
22 [84]	0.13	1.50	0.55	rVAChT-PC12 cell

Table 4: Accumulation of enantiomers of vesamicol analogs (**1**–**18**) in the striatum and cortex and the ratio of the striatum to cortex (ST/CTX) for enantiomers of radiolabeled vesamicol analogs.

	%ID/g			ST/CTX	Animal
	Cortex	Striatum	Whole brain		
(−)-[^{125}I]IBVM (**1**) [36]	2.56 (240 min)	6.26 (240 min)	—	2.44	Mouse
(+)-[^{125}I]IBVM (**1**) [36]	0.12 (240 min)	0.26 (240 min)	—	2.17	Mouse
(−)-[^{18}F]FEOBV (**2**)* [45]	4.5 (180 min)	9.0 (180 min)	—	1.74	Mouse
(+)-[^{18}F]FEOBV (**2**)* [45]	2.0 (180 min)	1.9 (45 min)	—	0.95	Mouse
(−)-[^{11}C]MABV (**3**)	3.99 (45 min)	8.1 (45 min)	—	2.03	Mouse
(+)-[^{11}C]MABV (**3**)	0.91 (45 min)	1.23 (45 min)	—	1.35	Mouse
(−)-[^{125}I]MIBT (**8**) [52]	—	—	0.27 (60 min)	—	Rat
(+)-[^{125}I]MIBT (**8**) [52]	—	—	0.83 (60 min)	—	Rat
(−)-[^{18}F]FBT (**9**) [57]	1.18 (60 min)	1.03 (60 min)	1.05 (60 min)	0.87	Rat
(+)-[^{18}F]FBT (**9**) [57]	0.58 (60 min)	0.74 (60 min)	0.59 (60 min)	1.28	Rat
(−)-[^{123}I]OIDV (**13**) [63]	0.62 (30 min)	0.63 (30 min)	—	1.02	Rat
(+)-[^{123}I]OIDV (**13**) [63]	0.46 (30 min)	0.45 (30 min)	—	0.98	Rat
(−)-[^{18}F]FBBV (**18**) [77]	—	—	0.226 (30 min)	—	Rat
(+)-[^{18}F]FBBV (**18**) [77]	—	—	0.071 (30 min)	—	Rat

*The value that was read from a graph was used.

analogs except for (−)-oIV (**10**) and (−)-OMV (**11**) may be caused by excretion of vesamicol analogs from brain by a P-glycoprotein related to the drug excretion mechanism or the high binding affinity for serum protein. The accumulation of (−)-[^{11}C]TZ659 (**20**) in the brain increased 2.2-fold by pretreatment with cyclosporine A (CycA), which inhibits a P-glycoprotein related to the drug excretion mechanism, 30 min prior to injection of a radiotracer. The vesamicol analogs except for (−)-oIV (**10**), (−)-OMV (**11**), and (−)-OIDV (**13**) showed a ratio of the striatum to cortex (ST/CTX) more than 1.1. As mentioned above, the VAChT-rich region was widely distributed in the various regions of the brain. These VAChT imaging agents will distribute in the cerebral cortex, the hippocampus, the thalamus, the hypothalamus, and the cerebellum besides the striatum. However, several vesamicol analogs showed the high concentration in the striatum and the low concentration in the cerebral cortex and the cerebellum.

3.4. The Influence of Enantioselectivity of Vesamicol Analogs on the In Vitro Binding Affinity for VAChT and In Vivo Brain Uptake. The influence of enantioselectivity of the vesamicol analogs FEOBV (**2**) [45], MIBT (**8**) [55], FBT (**9**) [60], oIV (**10**) [62], OMV (**11**) [63], OIDV (**13**) [67], FBBV (**18**) [78], **19** [81], TZ659 (**20**) [82], VAT (**21**) [83], and **22** [84] on the binding affinity for VAChT, σ_1, and σ_2 receptors was reported. The investigated vesmicol analogs except for MIBT (**8**) and FBT (**9**) showed that (−)-enantiomers had about 3- to 29-fold higher binding affinity for VAChT than (+)-enantiomers. MIBT (**8**) and FBT (**9**) showed that (+)-enantiomers had about 40- to 70-fold higher binding affinity for VAChT than (−)-enantiomers. On the contrary, several investigated vesamicol analogs such as oIV (**10**), OMV (**11**), and FBBV (**18**) showed that (−)-enantiomers had more than 3-fold lower binding affinity for σ_1 receptors than (+)-enantiomers (Table 3). The accumulation and retention of the investigated vesamicol analogs except for MIBT (**8**) in brain uptake showed that (−)-enantiomers had higher accumulation and retention in the brain than (+)-enantiomers. The accumulation ratios of the striatum to cortex (ST/CTX) of the investigated vesamicol analogs except for [^{18}F]FBT (**9**) showed that (−)-enantiomers were superior to (+)-enantiomers (Table 4).

3.5. The Structure-Activity Relationship of Radioligands for VAChT Imaging. In in vitro characterization, such as the affinity and selectivity of radioligands for VAChT, (−)-enantiomers of vesamicol analogs based on benzovesamicol ((−)-FEOBV (**2**) and (−)-FBBV (**18**)) are superior to other vesamicol analogs (Table 1). However, benzovesamicol analogs showed low brain uptake in the rat and mouse. On the contrary, in in vivo characterization, such as brain uptake of radioligands, vesamicol analogs that incorporated a radionuclide into the C ring of vesamicol ((−)-oIV (**10**) and (−)-OMV (**11**)) were superior to other vesamicol analogs (Table 2). However, (−)-oIV (**10**) and (−)-OMV (**11**) showed low selectivity for VAChT in vitro and in vivo. Considering abovementioned results, the in vivo characterization of radioligands for VAChT will improve by minimizing the molecular weight of the ligand, and in vitro characterization of radioligands for VAChT will improve by incorporating a carbonyl group between the B ring and C ring of vesamicol analogs. We are interested in vesamicol analogs incorporating three elements such as a carbonyl group between the B ring and C ring, a 4- to 7-membered alicyclic ring as A ring, and a radionuclide in the C ring, together.

4. Conclusion

Many vesamicol analogs were investigated as an VAChT imaging agent. In this report, 5 types of vesamicol analogs were investigated: (1) vesamicol analogs based on benzovesamicol, (2) vesamicol analogs based on trozamicol, (3) vesamicol analogs that incorporated a radionuclide into the C ring of vesamicol, (4) vesamicol analogs that incorporated alicyclic groups into the A ring of vesamicol, and (5) vesamicol analogs that incorporated a carbonyl group

between the B ring and C ring of benzovesamicol. All vesamicol analogs (**1**–**22**) are insufficient as an VAChT imaging agent for early diagnosis of Alzheimer's disease. This is because the vesamicol analogs with a high affinity and a high selectivity for VAChT showed low brain uptake, and vesamicol analogs with a high brain uptake showed high affinity for sigma receptors and low selectivity for VAChT. Considering the relationship between the cholinergic nerve system and AD, the development of a VAChT imaging agent is important. It is necessary that the suitable radioligand for VAChT imaging shows a high affinity and high selectivity for VAChT in vitro and in vivo and shows the high accumulation of the regional brain in accordance with the concentration distribution of VAChT in the brain. Furthermore, the ideal radioligand for VAChT imaging will require the fast blood clearance and the resistance to cleavage of the radioligand as described by Giboureau et al. previously. In the future, the suitable cholinergic neuronal degeneration imaging is thought to be found by comparing these three imaging: ChT imaging, VAChT imaging, and ChT imaging, and putting them together. It is necessary to further the development of a radioactive imaging agent for choline transporter (ChT) and choline acetyl transferase (ChAT). Finally, the ideal AD imaging is thought to be obtained by putting amyloid imaging, tau imaging, and cholinergic neuronal imaging together.

Conflicts of Interest

The authors declare that there are no conflicts of interest.

References

[1] H. A. Archer, P. Edison, D. J. Brooks et al., "Amyloid load and cerebral atrophy in Alzheimer's disease: an ^{11}C-PIB positron emission tomography study," *Annals of Neurology*, vol. 60, no. 1, pp. 145–147, 2006.

[2] J. Fripp, P. Bourgeat, O. Acosta et al., "Appearance modeling of ^{11}C PiB PET images: characterizing amyloid deposition in Alzheimer's disease, mild cognitive impairment and healthy aging," *NeuroImage*, vol. 43, no. 3, pp. 430–439, 2008.

[3] S. Hatashita and H. Yamasaki, "Clinically different stages of Alzheimer's disease associated by amyloid deposition with [^{11}C]-PIB PET imaging," *Journal of Alzheimer's Disease*, vol. 21, no. 3, pp. 995–1003, 2010.

[4] R. C. Petersen, H. J. Wiste, S. D. Weigand et al., "Association of elevated amyloid levels with cognition and biomarkers in cognitively normal people from the community," *JAMA Neurology*, vol. 73, no. 1, pp. 85–92, 2015.

[5] M. R. Brier, J. E. McCarthy, T. L. S. Benzinger et al., "Local and distributed PiB accumulation associated with development of preclinical Alzheimer's disease," *Neurobiology of Aging*, vol. 38, pp. 104–111, 2016.

[6] V. L. Villemagne, R. S. Mulligan, S. Pejoska et al., "Comparison of ^{11}C-PiB and ^{18}F-florbetaben for Abeta imaging in ageing and Alzheimer's disease," *European Journal of Nuclear Medicine and Molecular Imaging*, vol. 39, no. 6, pp. 983–989, 2012.

[7] H. Barthel, H. J. Gertz, S. Dresel et al., "Cerebral amyloid-beta PET with florbetaben ((18)F) in patients with Alzheimer's disease and healthy controls: a multicenter phase 2 diagnostic study," *The Lancet Neurology*, vol. 10, no. 5, pp. 424–35, 2011.

[8] V. L. Villemagne, K. Ong, R. S. Mulligan et al., "Amyloid imaging with ^{18}F-florbetaben in Alzheimer disease and other dementias," *Journal of Nuclear Medicine*, vol. 52, no. 8, pp. 1210–1217, 2011.

[9] K. T. Ong, V. L. Villemagne, A. Bahar-Fuchs et al., "Abeta imaging with ^{18}F-florbetaben in prodromal Alzheimer's disease: a prospective outcome study," *Journal of Neurology, Neurosurgery, and Psychiatry*, vol. 86, no. 4, pp. 431–436, 2015.

[10] O. Sabri, M. N. Sabbagh, J. Seibyl et al., "Florbetaben PET imaging to detect amyloid beta plaques in Alzheimer's disease: phase 3 study," *Alzheimer's & Dementia*, vol. 11, no. 8, pp. 964–974, 2015.

[11] C. C. Rowe, K. A. Ellis, M. Rimajova et al., "Amyloid imaging results from the Australian Imaging, Biomarkers and Lifestyle (AIBL) study of aging," *Neurobiology of Aging*, vol. 31, no. 8, pp. 1275–1283, 2010.

[12] P. V. Arriagada, J. H. Growdon, E. T. Hedley-Whyte, and B. T. Hyman, "Neurofibrillary tangles but not senile plaques parallel duration and severity of Alzheimer's disease," *Neurology*, vol. 42, no. 3, pp. 631–639, 1992.

[13] L. M. Bierer, P. R. Hof, D. P. Purohit, L. Carlin, J. Schmeidler, and K. L. Davis, "Neocortical neurofibrillary tangles correlate with dementia severity in Alzheimer's disease," *Archives of Neurology*, vol. 52, no. 1, pp. 81–88, 1995.

[14] T. Gomez-Isla, R. Hollister, H. West, S. Mui, J. H. Growdon, and R. C. Petersen, "Neuronal loss correlates with but exceeds neurofibrillary tangles in Alzheimer's disease," *Annals of Neurology*, vol. 41, no. 1, pp. 17–24, 1997.

[15] D. A. Bennett, J. A. Schneider, Z. Arvanitakis et al., "Neuropathology of older persons without cognitive impairment from two community-based studies," *Neurology*, vol. 66, no. 12, pp. 1837–1844, 2006.

[16] M. Maruyama, H. Shimada, T. Suhara et al., "Imaging of tau pathology in a tauopathy mouse model and in Alzheimer patients compared to normal controls," *Neuron*, vol. 79, no. 6, pp. 1094–1108, 2013.

[17] K. Shoghi-Jadid, G. W. Small, E. D. Agdeppa et al., "Localization of neurofibrillary tangles and beta-amyloid plaques in the brains of living patients with Alzheimer's disease," *American Journal of Geriatric Psychiatry*, vol. 10, no. 1, pp. 24–35, 2002.

[18] N. Okamura, S. Furumoto, R. Harada et al., "Novel ^{18}F-labeled arylquinoline derivatives for noninvasive imaging of tau pathology in Alzheimer's disease," *Journal of Nuclear Medicine*, vol. 54, no. 8, pp. 1420–1427, 2013.

[19] M. Shidahara, B. A. Thomas, N. Okamura et al., "A comparison of five partial volume correction methods for tau and amyloid PET imaging with [^{18}F]THK5351 and [^{11}C]PIB," *Annals of Nuclear Medicine*, vol. 31, no. 7, pp. 563–569, 2017.

[20] D. T. Chien, A. K. Szardenings, S. Bahri et al., "Early clinical PET imaging results with the novel PHF-tau radioligand [^{18}F]-T808," *Journal of Alzheimer's Disease*, vol. 38, no. 1, pp. 171–184, 2014.

[21] C. R. Jack, D. S. Knopman, W. J. Jagust et al., "Hypothetical model of dynamic biomarkers of the Alzheimer's pathological cascade," *The Lancet Neurology*, vol. 9, no. 1, pp. 119–128, 2010.

[22] C. Holmes, D. Boche, D. Wilkinson et al., "Long-term effects of Aβ42 immunisation in Alzheimer's disease: follow-up of a randomized, placebo-controlled phase I trial," *The Lancet*, vol. 372, no. 9634, pp. 216–223, 2008.

[23] P. Raina, P. Santaguida, A. Ismaila et al., "Effectiveness of cholinesterase inhibitors and memantine for treating dementia: evidence review for a clinical practice guideline," *Annals of Internal Medicine*, vol. 148, no. 5, pp. 379–397, 2008.

[24] Y. Sun, M. S. Lai, C. J. Lu, and R. C. Chen, "How long can patients with mild or moderate Alzheimer's dementia maintain both the cognition and the therapy of cholinesterase inhibitors: a national population-based study," *European Journal of Neurology*, vol. 15, no. 3, pp. 278–283, 2008.

[25] R. T. Bartus, "On neurodegenerative disease, models, and treatment strategies: lessons learned and lessons forgotten a generation following the cholinergic hypothesis," *Experimental Neurology*, vol. 163, no. 2, pp. 495–529, 2000.

[26] P. L. McGeer, "Aging, Alzheimer's disease, and the cholinergic system," *Canadian Journal of Physiology and Pharmacology*, vol. 62, no. 7, pp. 741–754, 1984.

[27] K. J. Reinikainen, H. Soininen, and P. J. Riekkinen, "Neurotransmitter changes in Alzheimer's disease: implications to diagnostics," *Journal of Neuroscience Research*, vol. 27, no. 4, pp. 576–586, 1990.

[28] T. Irie, K. Fukushi, Y. Akimoto, H. Tamagami, and T. Nozaki, "Design and evaluation of radioactive acetylcholine analogs for mapping brain acetylcholinesterase (AChE) in vivo," *Nuclear Medicine and Biology*, vol. 21, no. 6, pp. 801–808, 1994.

[29] D. E. Kuhl, R. A. Koeppe, S. Minoshima et al., "In vivo mapping of cerebral acetylcholinesterase activity in aging and Alzheimer's disease," *Neurology*, vol. 52, no. 4, pp. 691–699, 1999.

[30] N. I. Bohnen, D. I. Kaufer, R. Hendrickson et al., "Cognitive correlates of alterations in acetylcholinesterase in Alzheimer's disease," *Neuroscience Letters*, vol. 380, no. 1-2, pp. 127–132, 2005.

[31] H. Namba, M. Iyo, H. Shinotoh, S. Nagatsuka, K. Fukushi, and T. Irie, "Preserved acetylcholinesterase activity in aged cerebral cortex," *The Lancet*, vol. 351, no. 9106, pp. 881-882, 1998.

[32] J. Pascual, A. Fontan, J. J. Zarranz, J. Beeciano, J. Florez, and A. Pazos, "High-affinity choline uptake carrier in Alzheimer's disease: implications for the cholinergic hypothesis of dementia," *Brain Research*, vol. 552, no. 1, pp. 170–174, 1991.

[33] B. A. Bar and S. M. Parsons, "Demonstration of a receptor in *Torpedo* synaptic vesicles for the acetylcholine storage blocker L-*trans*-2-(4-phenyl[3,4-3H]-piperidino)cyclohexanol," *Proceedings of the National Academy of Sciences of the United States of America*, vol. 83, no. 7, pp. 2267–2270, 1986.

[34] I. G. Marshall and S. M. Parsons, "The vesicular acetylcholine transport system," *Trends in Neurosciences*, vol. 10, no. 4, pp. 174–177, 1987.

[35] N. Giboureau, I. M. Som, A. B. Arnold, D. Duilloteau, and M. Kassiou, "PET radioligands for the vesicular acetylcholine transporter (VAChT)," *Current Topics in Medicinal Chemistry*, vol. 10, no. 15, pp. 1569–1583, 2010.

[36] G. A. Rogers, S. M. Parsons, D. C. Anderson et al., "Synthesis, in vitro acetylcholine-storage-blocking activities, and biological properties of derivatives and analogues of *trans*-2-(4-phenylpiperidino)cyclohexanol(vesamicol)," *Journal of Medicinal Chemistry*, vol. 32, no. 6, pp. 1217–1230, 1989.

[37] Y. W. Jung, M. E. Van Dort, D. L. Gildersleeve, and D. M. Wieland, "A radiotracer for mapping cholinergic neurons of the brain," *Journal of Medicinal Chemistry*, vol. 33, no. 8, pp. 2065–2068, 1990.

[38] M. E. Van Dort, Y. W. Jung, D. L. Gildersleeve, C. A. Hagen, D. E. Kuhl, and D. M. Wieland, "Synthesis of 123I- and 125I-labeled cholinergic nerve marker (−)-5-iodobenzovesamicol," *Nuclear Medicine and Biology*, vol. 20, no. 8, pp. 929–937, 1993.

[39] D. E. Kuhl, R. A. Koeppe, J. A. Fessler et al., "In vivo mapping of cholinergic neurons in the human brain using SPECT and IBVM," *Journal of Nuclear Medicine*, vol. 35, no. 3, pp. 405–410, 1994.

[40] D. E. Kuhl, S. Minoshima, J. A. Fessler et al., "In vivo mapping of cholinergic terminals in normal aging, Alzheimer's disease, and Parkinson's disease," *Annals of Neurology*, vol. 40, no. 3, pp. 399–410, 1996.

[41] Y. W. Jung, K. A. Frey, G. K. Mulholland et al., "Vesamicol receptor mapping of brain cholinergic neurons with radioiodine labeled positional isomers of benzovesamicol," *Journal of Medicinal Chemistry*, vol. 39, no. 17, pp. 3331–3342, 1996.

[42] D. Sorger, R. Schliebs, I. Kampfer et al., "In vivo [^{125}I]-iodobenzovesamicol binding reflects cortical cholinergic deficiency induced by specific immunolesion of rat basal forebrain cholinergic system," *Nuclear Medicine and Biology*, vol. 27, no. 1, pp. 23–31, 2000.

[43] J. Mazere, C. Prunier, O. Barret et al., "In vivo SPECT imaging of vesicular acetylcholine transporter using [^{123}I]-IBVM in early Alzheimer's disease," *NeuroImage*, vol. 40, no. 1, pp. 280–288, 2008.

[44] G. K. Mulholland, Y. W. Jung, D. M. Wieland, M. R. Kilbourn, and D. E. Kuhl, "Synthesis of [^{18}F]fluoroethoxy-benzobesamicol, a radiotracer for cholinergic neurons," *Journal of Labelled Compounds and Radiopharmaceuticals*, vol. 33, no. 7, pp. 583–591, 1993.

[45] M. Kovac, S. Mavel, W. D. Conrad et al., "3D QSAR study, synthesis, and in vitro evaluation of (+)-5-FBVM as potential PET radioligand for the vesicular acetylcholine transporter (VAChT)," *Bioorganic & Medicinal Chemistry*, vol. 18, no. 21, pp. 7659–7667, 2010.

[46] G. K. Mulholland, D. M. Wieland, M. R. Kilbourn et al., "[^{18}F] fluoroethoxy-benzovesamicol, a PET radiotracer for the vesicular acetylcholine transporter and cholinergic synapses," *Synapse*, vol. 30, no. 3, pp. 263–274, 1998.

[47] M. Petrou, K. A. Frey, M. R. Kilbourn et al., "In vivo imaging of human cholinergic nerve terminals with (-)-5-^{18}F-fluoroethoxybenzovesamicol: biodistribution, dosimetry, and tracer kinetic analyses," *Journal of Nuclear Medicine*, vol. 55, no. 3, pp. 396–404, 2014.

[48] M. R. Kilbourn, Y.-W. Jung, M. S. Haka, D. L. Gildersleeve, D. E. Kuhl, and D. M. Wieland, "Mouse brain distribution of a carbon-11 labeled vesamicol derivative: presynaptic marker of cholinergic neurons," *Life Sciences*, vol. 47, no. 21, pp. 1955–1963, 1990.

[49] G. A. Rogers, S. Stone-Elander, M. Ingvar, L. Eriksson, S. M. Persons, and L. Widen, "^{18}F-labeled vesamicol derivatives: syntheses and preliminary in vitro small animal positron emission tomography evaluation," *Nuclear Medicine and Biology*, vol. 21, no. 2, pp. 219–230, 1994.

[50] M. Ingvar, S. Stone-Elander, G. A. Rogers, B. Johansson, L. Eriksson, and S. M. Persons, "Striatal D2/acetylcholine interactions: PET studies of the vesamicol receptor," *NeuroReport*, vol. 4, no. 12, pp. 1311–1314, 1993.

[51] K. Bando, K. Taguchi, Y. Ginoza et al., "Synthesis and evaluation of radiolabeled piperazine derivatives of vesamicol as SPECT agents for cholinergic neurons," *Nuclear Medicine and Biology*, vol. 28, no. 3, pp. 251–260, 2001.

[52] S. Nishiyama, H. Ohba, T. Kobayashi et al., "Development of novel PET probe [^{11}C](R,R)HAPT and its stereoisomer [^{11}C](S,S)HAPT for vesicular acetylcholine transporter imaging: a PET study in conscious monkey," *Synapse*, vol. 68, no. 7, pp. 283–292, 2014.

[53] C. Barthel, D. Sorger, W. D. Conrad et al., "New systematically modified vesamicol analogs and their affinity and selectivity for the vesicular acetylcholine transporter–a critical examination

of the lead structure," *European Journal of Nuclear Medicine and Molecular Imaging*, vol. 100, pp. 50–67, 2015.

[54] S. M. N. Efange, R. H. Mach, C. R. Smith et al., "Vesamicol analogues as sigma ligands: molecular determinants of selectivity at the vesamicol receptor," *Biochemical Pharmacology*, vol. 49, no. 6, pp. 791–797, 1995.

[55] F. G. J. Custers, J. E. Leysen, J. C. Stoof, and J. D. M. Herscheid, "Vesamicol and some of its derivatives: questionable in rat brain," *European Journal of Pharmacology*, vol. 338, no. 2, pp. 177–183, 1997.

[56] S. M. N. Efange, R. H. Michelson, A. B. Khare, and J. R. Thomas, "Synthesis and tissue distribution of (m-[^{125}I] iodobenzyl)trozamicol ([^{125}I]MIBT): potential radioligand for mapping central cholinergic innervation," *Journal of Medicinal Chemistry*, vol. 36, no. 12, pp. 1754–1760, 1993.

[57] S. M. N. Efange, R. B. Langason, A. B. Khare, and W. C. Low, "The vesamicol receptor ligand (+)-meta-[^{125}I]iodobenzyltrozamicol [(+)-[^{125}I]-MIBT] reveals blunting of the striatal cholinergic response to dopamine D2 receptor blockade in the 6-hydroxydopamine (6-OHDA)-lesioned rat: possible implications for Parkinson's disease," *Life Sciences*, vol. 58, no. 16, pp. 1367–1374, 1996.

[58] J. K. Staley, D. C. Mash, S. M. Persons, A. B. Khare, and S. M. N. Efange, "Pharmacological characterization of the vesamicol analogue (+)-[^{125}I]MIBT in primate brain," *European Journal of Pharmacology*, vol. 338, no. 2, pp. 159–169, 1997.

[59] R. M. Baldwin, M. Al-Tikriti, Y. Zea-Ponce et al., "Synthesis and monkey SPECT imaging of the putative vesamicol receptor binding radiotracer [^{123}I]MIBT," *Journal of Nuclear Medicine*, vol. 38, p. 181P, 1997.

[60] R. H. Mach, M. L. Voytko, R. L. E. Ehrenkaufer et al., "Imaging of cholinergic terminals using the radiotracer: [^{18}F] (+)-4-fluorobenzotrozamicol: in vitro binding studies and positron emission tomography studies in nonhuman primates," *Synapse*, vol. 25, no. 4, pp. 368–380, 1997.

[61] H. D. Gage, M. L. Voytko, R. L. E. Ehrenkaufer, J. R. Tobin, S. M. N. Efange, and R. H. Mach, "Reproducibility of repeated measures of cholinergic terminal density using [^{18}F] (+)-4-fluorobenzyltrozamicol and PET in the rhesus monkey brain," *Journal of Nuclear Medicine*, vol. 41, no. 12, pp. 2069–2076, 2000.

[62] K. Shiba, T. Yano, W. Sato, H. Mori, and N. Tonami, "Characterization of radioiodinated (−)-ortho-iodovesamicol binding in rat brain preparations," *Life Sciences*, vol. 71, no. 13, pp. 1591–1598, 2002.

[63] K. Shiba, K. Ogawa, K. Ishiwata, K. Yajima, and H. Mori, "Synthesis and binding affinities of methylvesamicol analogs for the acetylcholine transporter and sigma receptor," *Bioorganic & Medicinal Chemistry*, vol. 14, no. 8, pp. 2620–2626, 2006.

[64] S. M. N. Efange, K. von Hohenberg, A. B. Khare, Z. Tu, R. H. Mach, and S. M. Parsons, "Synthesis and biological characterization of stable and radioiodinated *trans*-2-hydroxy-3-[4-(3-iodophenyl)piperidyl]-1,2,3,4-tetrahydronaphthalene (3′-IBVM)," *Nuclear Medicine and Biology*, vol. 27, no. 8, pp. 749–755, 2000.

[65] T. Kozaka, I. Uno, Y. Kitamura, D. Miwa, K. Ogawa, and K. Shiba, "Syntheses and in vitro evaluation of decalinvesamicol analogues as potential imaging probes for vesicular acetylcholine transporter (VAChT)," *Bioorganic & Medicinal Chemistry*, vol. 20, no. 16, pp. 4936–4941, 2012.

[66] I. Uno, T. Kozaka, D. Miwa et al., "In vivo differences between two optical isomers of radioiodinated *o*-iodo-*trans*-decalinvesamicol for use as a radioligand for the vesicular acetylcholine transporter," *PLoS One*, vol. 11, no. 1, Article ID e0146719, 2016.

[67] M. A. Azim, T. Kozaka, I. Uno et al., "The potential of *o*-bromo-*trans*-decalinvesamicol as a new PET ligand for vesicular acetylcholine transporter imaging," *Synapse*, vol. 68, no. 10, pp. 445–453, 2014.

[68] Y. Kitamura, T. Kozaka, D. Miwa et al., "Synthesis and evaluation of a new vesamicol analog *o*-[^{11}C]methyl-*trans*-decalinvesamicol as a PET ligand for the vesicular acetylcholine transporter," *Annals of Nuclear Medicine*, vol. 30, no. 2, pp. 122–129, 2016.

[69] D. Sorger, M. Scheunemann, U. Grossmann et al., "A new 18F labeled fluoroacetylmorpholino derivative of vesamicol for neuroimaging of the vesicular acetylcholine transporter," *Nuclear Medicine and Biology*, vol. 35, no. 2, pp. 185–195, 2008.

[70] D. Sorger, M. Scheunemann, J. Vercouille et al., "Neuroimaging of the vesicular acetylcholine transporter by a novel 4-[18F]fluoro-benzoyl derivative of 7-hydroxy-6-(4-phenylpiperidin-1-yl)-octahydro-benzo[1,4]oxazines," *Nuclear Medicine and Biology*, vol. 36, no. 1, pp. 17–27, 2009.

[71] Z. Tu, S. M. N. Efange, J. Xu et al., "Synthesis and in vitro and in vivo evaluation of 18F-labeled positron emission tomography (PET) ligands for imaging the vesicular acetylcholine transporter," *Journal of Medicinal Chemistry*, vol. 52, no. 5, pp. 1358–1369, 2009.

[72] S. M. N. Efange, R. H. Mach, A. B. Khare, R. H. Michelson, P. A. Nowak, and P. H. Evora, "[^{18}F]fluorobenzyltrozamicol ([^{18}F]FBT): molecular decomposition-reconstitution approach to vesamicol receptor radioligands for positron emission tomography," *Applied Radiation and Isotopes*, vol. 45, no. 4, pp. 465–472, 1994.

[73] K. Shiba, H. Mori, H. Matsuda, S. Tsuji, N. Tonami, and K. Hisada, "In vivo characterization of radioiodinated 2-(4-phenylpiperidino)cyclohexanol (vesamicol) analogs: potential radioligand for mapping presynaptic cholinergic neurons," *Nuclear Medicine and Biology*, vol. 22, no. 6, pp. 823–828, 1995.

[74] K. Shiba, H. Mori, and N. Tonami, "Evaluation of radioiodinated (−)-*o*-iodovesamicol as a radiotracer for mapping the vesicular acetylcholine transporter," *Annals of Nuclear Medicine*, vol. 17, no. 6, pp. 451–456, 2003.

[75] K. Kawamura, K. Shiba, H. Tsukada, S. Nishiyama, H. Mori, and K. Ishiwata, "Synthesis and evaluation of vesamicol analog (−)-*o*-[^{11}C]methylvesamicol as a PET ligand for vesicular acetylcholine transporter," *Annals of Nuclear Medicine*, vol. 20, no. 6, pp. 417–424, 2006.

[76] K. Shiba, S. Nishiyama, H. Tsukada et al., "The potential of (−)-*o*-[^{11}C]methylvesamicol for diagnosing cholinergic deficit dementia," *Synapse*, vol. 63, no. 2, pp. 167–171, 2009.

[77] T. Kozaka, I. Uno, Y. Kitamura et al., "Regional brain imaging of vesicular acetylcholine transporter (VAChT) using *o*-[^{125}I] iodo-*trans*-decalinvesamicol as a new potential imaging probe," *Synapse*, vol. 68, no. 3, pp. 107–113, 2014.

[78] S. M. N. Efange, A. B. Khare, K. von Hohenberg, R. H. Mach, S. M. Parsons, and Z. Tu, "Synthesis and in vitro biological evaluation of carbonyl group-containing inhibitors of vesicular acetylcholine transporter," *Journal of Medicinal Chemistry*, vol. 53, no. 7, pp. 2825–2835, 2010.

[79] P. K. Padakanti, X. Zhang, J. Li, and S. M. Parsons, "Syntheses and radiosyntheses of two carbon-11 labeled potent and selective radioligands for mapping vesicular acetylcholine transporter," *Molecular Imaging and Biology*, vol. 16, no. 6, pp. 765–772, 2014.

[80] P. K. Padakanti, X. Zhang, H. Jin et al., "In vitro and in vivo characterization of two C-11 labeled PET tracer for vesicular acetylcholine transporter," *Molecular Imaging and Biology*, vol. 16, no. 6, pp. 773–780, 2014.

[81] J. Li, X. Zhang, Z. Zhang et al., "Heteroaromatic and aniline derivatives of piperidines as potent ligands for vesicular acetylcholine transporter," *Journal of Medicinal Chemistry*, vol. 56, no. 15, pp. 6216–6233, 2013.

[82] H. Jin, X. Zhang, H. Liu et al., "Kinetics modeling and occupancy studies of a novel C-11 PET tracer for VAChT in nonhuman primates," *Nuclear Medicine and Biology*, vol. 43, no. 2, pp. 131–139, 2016.

[83] Z. Tu, X. Zhang, H. Jin et al., "Synthesis and biological characterization of a promising F-18 PET tracer for vesicular acetylcholine transporter," *Bioorganic & Medicinal Chemistry*, vol. 23, no. 15, pp. 4699–4709, 2015.

[84] X. Yue, H. Jin, H. Liu et al., "Synthesis, resolution, and in vitro evaluation of three vesicular acetylcholine transporter ligands and evaluation of the fluorine-18 radioligand in a nonhuman primate," *Organic and Biomolecular Chemistry*, vol. 15, no. 24, pp. 5197–5209, 2017.

[85] D. M. Armstrong, C. B. Saper, A. I. Levey, B. H. Wainer, and R. D. Terry, "Distribution of cholinergic neurons in rat brain: demonstrated by the immunocytochemical localization of choline acetyltransferase," *Journal of Comparative Neurology*, vol. 216, no. 1, pp. 53–68, 1983.

[86] L. L. Butcher and N. J. Woolf, "Cholinergic neurons and networks revisited," in *The Rat Nervous System*, Paxions, Ed., pp. 1257–1268, Elsvier Academic Press, San Diego, CA, USA, 3rd edition, 2004.

[87] C. R. Houser, G. D. Crawford, R. P. Barber, P. M. Salvaterra, and J. E. Vaughn, "Organization and morphological characteristics of cholinergic neurons: an immunocytochemical study with a monoclonal antibody to choline acetyltransferase," *Brain Research*, vol. 266, no. 1, pp. 97–119, 1983.

[88] H. Kimura, P. L. McGeer, J. H. Peng, and E. G. McGeer, "The central cholinergic system studied by choline acetyltransferase immunohistochemistry in the cat," *Journal of Comparative Neurology*, vol. 200, no. 2, pp. 151–201, 1981.

[89] K. Semba and H. C. Fibiger, "Organization of central cholinergic systems," *Progress in Brain Research*, vol. 79, pp. 37–63, 1989.

[90] N. J. Woolf, "Cholinergic systems in mammalian brain and spinal cord," *Progress in Brain Research*, vol. 37, no. 6, pp. 475–524, 1991.

[91] A. David and A. McCormick, *Acetylcholine: Distribution, Receptors, and Actions. Section of Neuroanatomy*, Yale Univrersity of School of Medicine, New Haven, CT, USA, 1989.

[92] R. Quirion, I. Aubert, D. M. Araujo, A. Hersi, and P. Gaudreau, "Autoradiographic distribution of putative muscarinic receptor sub-types in mammalian brain," *Progress in Brain Research*, vol. 98, pp. 85–93, 1993.

[93] I. L. Allan, A. K. Cheryl, F. S. Willium, L. P. Donald, and P. B. Mark, "Identification and localization of muscarinic acetylcholine receptor proteins in brain with subtype-specific antibodies," *Journal of Neuroscience*, vol. 11, no. 10, pp. 3218–3226, 1991.

[94] A. Rotter and D. M. Jacobwitz, "Neurochemical identification of cholinergic forebrain projection sites of the nucleus tegmentalis dorsalis lateralis," *Brain Research Bulletin*, vol. 6, no. 4-6, pp. 525–529, 1981.

[95] J. Mensch, J. Oyarzabal, C. Mackie, and P. Augustings, "In vivo, in vitro and in silico methods for small molecule transfer across the BBB," *Journal of Pharmaceutical Sciences*, vol. 98, no. 12, pp. 4429–4468, 2009.

[96] H. Pajouhesh and G. R. Lenz, "Medicinal chemical properties of successful central nervous system drugs," *NeuroRX*, vol. 2, no. 4, pp. 541–553, 2005.